JOURNAL OF BACTERIOLOGY, Jan. 2010, p. 568–574 Vol. 192, No. 2
0021-9193/10/$12.00 doi:10.1128/JB.01049-09

The Aromatic Ring of Phenylalanine 334 Is Essential for Oligomerization of *Vibrio vulnificus* Hemolysin[▽]

Takashige Kashimoto,* Shunji Ueno, Takeshi Koga, Shinji Fukudome, Hayato Ehara, Mayumi Komai, Hiroyuki Sugiyama, and Nobuyuki Susa

Laboratory of Veterinary Public Health, School of Veterinary Medicine, Kitasato University, Higashi 23-35-1, Towada Aomori 034-8628, Japan

Received 10 August 2009/Accepted 8 October 2009

Vibrio vulnificus **hemolysin (VVH) is thought to be a member of the cholesterol-dependent cytolysin (CDC) family of pore-forming toxins. To date, the structure-function relationships of CDCs produced by Gram-negative bacteria remain largely unknown. We show here that the aromatic ring of phenylalanine residue conserved in *Vibrionaceae* hemolysins is essential for oligomerization of VVH. We generated the VVH mutants; substituted Phe 334 for Ile (F334I), Ala (F334A), Tyr (F334Y), or Trp (F334W); and tested their binding and oligomerizing activity on Chinese hamster ovary cells. Binding in all mutants fell by approximately 50% compared with that in the wild type. Oligomerizing activities were completely eliminated in F334I and F334A mutants, whereas this ability was partially retained in F334Y and F334W mutants. These findings indicate that both hydrophobicity and an aromatic ring residue at the 334th position were needed for full binding activity and that the oligomerizing activity of this toxin was dependent on the existence of an aromatic ring residue at the 334th position. Our findings might help further understanding of the structure-and-function relationships in *Vibrionaceae* hemolysins.**

Vibrio vulnificus hemolysin (VVH) is a pore-forming toxin produced by the Gram-negative bacterium *Vibrio vulnificus* (6, 11). VVH binds directly to cholesterol and is oligomerized *in vitro*. Once VVH forms the VVH-cholesterol complex, it can no longer bind to susceptible cells (10). Therefore, VVH could be considered a member of the cholesterol-dependent cytolysin (CDC) toxin family (35).

A wide variety of Gram-positive and some Gram-negative bacteria produce CDCs, which require cellular cholesterol to exert their cytotoxicity (22, 38). Structure-function relationships between CDCs produced by Gram-positive bacteria (gpCDCs) have been studied intensively for over a decade, whereas CDCs produced by Gram-negative bacteria remain largely unknown. On the other hand, it is well known that some *Vibrionaceae* bacteria, such as *Vibrio vulnificus*, *Vibrio cholerae*, *Aeromonas hydrophila*, and *Aeromonas sobria*, produce pore-forming toxins/hemolysins. Among them, it was reported that VVH and *Vibrio cholerae* cytolysin (VCC) required cholesterol to exert their activity (12, 35). Thus, *Vibrionaceae* hemolysins are thought to be members of the CDC family. The generalized toxic steps are thought to be similar for both gpCDCs and *Vibrionaceae* hemolysins (22); i.e., monomers interact with a susceptible cell membrane, these monomers are assembled to form oligomers by membrane fluidity, and transmembrane pore formation follows (5, 22, 27, 30, 37). Although gpCDCs and *Vibrionaceae* hemolysins have common toxic steps, the following differences exist between them. (i) There is no similarity in amino acid sequences. (ii) gpCDCs have a highly conserved tryptophan-rich motif, which is involved in membrane recognition (3, 9, 27), whereas this motif does not exist in *Vibrionaceae* hemolysins. (iii) gpCDCs, such as perfringolysin and intermedilicine, are composed of four domains, whereas *Vibrionaceae* hemolysins are composed of two or three domains (21, 24, 25). (iv) *Vibrionaceae* hemolysins form pores that are smaller (2 to 3 nm in diameter) (33, 36) than those formed by gpCDCs (approximately 30 nm) (1, 2, 19).

Recently, the crystal structure of VCC was determined (21). VCC is composed of three domains, namely the cytolysin domain, the β-trefoil lectin domain, and the β-prism lectin domain (21). The proposed mechanisms of action of VCC are as follows: (i) monomer binding to cell surfaces via interactions with the cytolysin domain, (ii) binding to carbohydrate receptors by the β-prism lectin domain, (iii) oligomerization via the cytolysin domain, and (iv) pore formation by insertion of a stem-loop from the cytolysin domain into the cellular membrane (21). On the other hand, from the analysis of the VVH amino acid sequence, it has been predicted that VVH is composed of two domains (21) and is missing the β-prism lectin domain, which binds to carbohydrate receptors on the cellular membrane (21). Therefore, the structure and functions of VVH are thought to be slightly different from those of VCC. Thus, analysis of the structure-function relationship of VVH will aid in the understanding of the evolutionary process of CDCs as well as of the toxic mechanism of VVH.

In this study, we show that phenylalanine in the 334th position (F334) is required for the binding and oligomerizing ability of VVH. In particular, the benzene ring of this phenylalanine is a prerequisite for its oligomerizing ability. Because of the high conservation of this phenylalanine in other *Vibrionaceae* hemolysins, our results will contribute to a better understanding of the structure-function relationships of *Vibrionaceae* hemolysins.

* Corresponding author. Mailing address: Laboratory of Veterinary Public Health, School of Veterinary Medicine, Kitasato University, Higashi 23-35-1, Towada-shi, Aomori-ken 034-8628, Japan. Phone: 81 176 23 4371, ext. 443. Fax: 81 176 23 8703. E-mail: kashimot@vmas.kitasato-u.ac.jp.

▽ Published ahead of print on 6 November 2009.

MATERIALS AND METHODS

Cell culture. Chinese hamster ovary (CHO) cells were grown in Dulbecco's modified Eagle's minimum essential medium (DMEM; Gibco BRL Life Technologies, Rockville, MD) supplemented with 2 mM glutamine, 2 mM sodium pyruvate, and 10% heat-treated fetal calf serum. Cells were incubated at 37°C under 5% CO_2 in air in a humidified atmosphere.

Construction, expression, and purification of recombinant VVHs. The Qiagen genomic tip (Qiagen, Hilden, Germany) was used for purification of genome DNA as recommended by the manufacturer. VVH-encoding gene *vvhA* was amplified without signal sequence by PCR with the primers 5′-CATATGCAA GAATATGTGCCGATTGTT-3′ (the underline indicates an NdeI site) and 5′-CTCGAGGAGTTTGACTTGTTGTAATGT-3′ (the underline indicates an XhoI site), from the *Vibrio vulnificus* genome as the template. The amplified DNA was ligated to the pGEM-T vector (Promega, Madison, WI), and the sequence was confirmed by DNA sequencing. The NdeI and XhoI fragment of this plasmid was inserted into pET29b (Novagen, Inc., Madison, WI) NdeI-XhoI site. The resultant plasmid was designated p*vvhA wt*. p*vvhA wt* was introduced into *Escherichia coli* JM109(DE3). The bacteria were cultivated in Luria-Bertani (LB) broth containing 10 μg of kanamycin/ml until an optical density at 600 nm of 0.6 was reached at 37°C, and then they were induced to produce the His-tagged protein by adding 0.1 mM isopropyl-β-D-thiogalactopyranoside (IPTG) at 20°C for 16 h. After induction of the protein, the bacteria were suspended with the binding buffer (5 mM imidazole, 500 mM NaCl, 20 mM Tris-HCl, pH 7.9). The bacterial suspension was sonicated using a Vibra Ultrasonic (model VCX-500; Sonics and Materials Inc., United States) and centrifuged at 21,000 × *g* at 4°C for 20 min. The supernatant was used for purification of His-tagged VVH. The His-tagged VVH was purified with His-Bind resin according to the manufacturer's instructions (Merck Biosciences, Darmstadt, Germany). After purification, His-tagged VVH was dialyzed with 10 mM glycine-NaOH, pH 9.8, and 200 mM NaCl. The protein concentrations were determined by the methods of Lowry et al. (15) and densitometry on sodium dodecyl sulfate-polyacrylamide gel electrophoresis (SDS-PAGE) gels with bovine serum albumin standard.

Random mutagenesis. Error-prone PCR was performed essentially as described by Fromant et al. (4) using $MnCl_2$ at a final concentration of 100 μM to facilitate mutation with p*VvhA wt* as the template. Reactions were subjected to 20 cycles with the primers, 5′-CATATGCAAGAATATGTGCCGATTGTT-3′ and 5′-CTCGAGGAGTTTGACTTGTTGTAATGT-3′, under the following conditions: 94°C for 30 s; 51°C for 30 s; and 72°C for 3 min. After PCR amplification, the PCR product was purified using a gel extraction kit (Qiagen) and digested with NdeI and XhoI. This digested fragment was ligated into the NdeI and XhoI site of pET29b and then transformed into the competent cells. The expressed proteins were purified, and the cytopathic effect (CPE) on CHO cells was determined. The mutation site was identified by DNA sequencing.

Site-directed mutagenesis. A QuikChange (Stratagene, La Jolla, CA) site-directed mutagenesis kit was used. Various mutagenic primers were designed individually according to the desired mutations. The cycling parameters for the mutagenesis reactions were chosen based on the protocol suggested by the manufacturer. After PCR amplification, the reaction mixture was digested with 10 units of the restriction enzyme DpnI for 1 h. Competent cells were transformed by addition of 10 μl of DpnI-treated reaction mixture. Plasmid DNA was purified using the Qiagen plasmid purification kit (Qiagen, Valencia, CA). The desired mutation was confirmed by DNA sequencing.

Production of antibodies against VVH in rabbit. Fifteen-week-old New Zealand White rabbits were immunized subcutaneously with purified wild type (WT) in complete Freund's adjuvant (Difco, Detroit, MI) on day 0. On days 14 and 28, the same rabbits were given booster shots of the same antigen in Freund's incomplete adjuvant (Difco). Immune rabbit serum samples were collected 10 days after the last immunization. Immunoglobulin G (IgG) was purified with an Affi-Gel protein A MAPS II kit (Bio-Rad, Hercules, CA). Reactivity of the purified IgG was confirmed by Western blot analysis against WT and native VVH. The purified IgG was designated anti-VVH polyclonal antibody.

Observation of the CPE. CHO cells were incubated with the native VVH, WT, or a series of F334 mutants at 37°C for 5 h. The cells were photographed using a Leica FW4000 (Leica Micro systems, Wetzlar, Germany) fitted to the Leica DMI6000 microscope, and images were processed for publication by using Adobe Photoshop 7.0.

Cytotoxicity assays. Cytotoxicity was determined by a lactate dehydrogenase (LDH) release assay. Cells were seeded in 24-well tissue culture plates at 1×10^5 cells/well. After 24 h, the cells were washed twice with Hanks balanced salt solution (HBSS [Nissui Pharmaceutical Co., Ltd., Tokyo, Japan]), which was then replaced with prewarmed DMEM. The indicated concentrations of the WT or a series of F334 mutants (see Fig. 2) were inoculated into the wells and incubated for 2 h at 37°C. After incubation, aliquots of medium samples (sample LDH) were assayed for LDH activity using pyruvate as a substrate. Cells treated with the VVH vehicle only (control LDH) were used to assess background LDH activity, and cells lysed with 0.5% Triton X-100 were used to represent total LDH activity. The percentage of LDH release was calculated as follows: (sample LDH − control LDH)/(total LDH − control LDH) × 100.

Measurement of binding toxin on CHO cells. CHO cells were seeded in a 90-mm tissue culture dish at 1.5×10^6 cells/dish. After 48 h, the cells were washed twice with HBSS, which was then replaced with DMEM. WT and the series of F334 mutants were added to a final concentration of 20 μg/ml into the dish and incubated at 4°C for 1 h. Only monomer could be detected at this temperature. The cells were washed twice with phosphate-buffered saline and lysed in a lysis buffer (25 mM Tris-HCl, pH 7.4; 150 mM NaCl; 1% Triton X-100). The protein concentrations of the lysates were normalized by the BCA protein assay reagent kit (Pierce, Rockford, IL) and then applied to SDS-PAGE at 38 μg/lane. The cell lysates were separated on 10% SDS-polyacrylamide gels and transferred to an Immobilon-P transfer membrane (Millipore Corporation, Bedford, MA) using the Bio-Rad Trans-Blot system. The membrane was blocked for 12 h in phosphate-buffered saline with 0.05% Tween 20, which contained 5% dry milk at 4°C. The presence of VVH (monomer) was detected using anti-VVH polyclonal antibody. Cellular actin was detected by anti-actin monoclonal antibody (Chemicon International Inc., Temecula, CA). Primary antibodies were detected using horseradish peroxidase-conjugated secondary antibodies and enhanced chemiluminescence (Amersham Biosciences, Buckinghamshire, United Kingdom). The band intensities of monomer and actin were analyzed by densitometry using a CS analyzer (ATTO Corporation, Tokyo, Japan). Binding activities were calculated by dividing the band intensity of monomer by that of actin.

Detection of oligomer on CHO cells. CHO cells were seeded in a 90-mm tissue culture dish at 1.5×10^6 cells/dish. After 48 h, the cells were washed twice with HBSS, which was then replaced with DMEM. WT and the series of F334 mutants were added to final concentrations of 10 μg/ml and 20 μg/ml, respectively. The cells were incubated with toxin at 37°C for 1 h. Detection of oligomer was performed by the same method described above in the section on the measurement of binding toxin.

Homology modeling and template toxin. The modeling was performed using the 3D-JIGSAW protein comparative modeling server (http://www.bmm.icnet.uk/servers/3djigsaw). VCC was used as the template. VCC and VVH share 28% identities and 46% positives in aligned amino acid sequences as determined by BLAST2. We are confident that these two proteins are truly homologous, because both proteins have a lectin domain and pore-forming domain in the same positions. The cysteine residues involved in the VCC disulfide bond are also conserved at the same position in VVH (32).

RESULTS

Generating a noncytopathic mutant of VVH. The WT showed a CPE in CHO cells similar to that of native VVH purified from the culture supernatant of *Vibrio vulnificus* (Fig. 1). To investigate the functional key amino acid of VVH, we performed a random mutagenesis analysis and screened for noncytopathic mutants. Using a CPE assay, one clone with no CPE was obtained (Fig. 1A). However, random mutagenesis sometimes generates unfavorable mutants because of a frameshift or generation of a stop codon within the open reading frame. Therefore, to determine whether this mutant toxin was expressed as full-length VVH or not, the six-His tag which is fused at the C-terminal end was detected using anti-His tag antibody. As shown in Fig. 1B, the noncytopathic mutant was found to be the same size as the WT by anti-His tag antibody and anti-VVH antibody (Fig. 1B). These data indicate that the noncytopathic mutant expressed full-length VVH. We analyzed the mutation site of this mutant by DNA sequence, and it was revealed that phenylalanine 334 (F334) was replaced by isoleucine. To reconfirm the loss of CPEs by this mutation, we generated a point mutant (substituting Phe334 for Ile) by site-directed mutagenesis, and this was designated the F334I mutant.

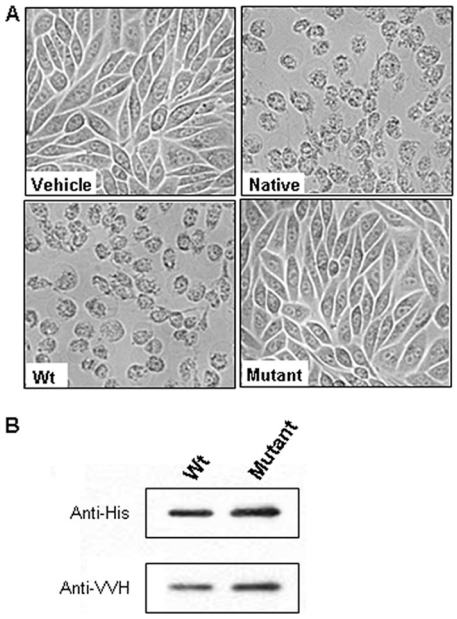

FIG. 1. Generation of noncytopathic mutant of VVH by random mutagenesis. (A) CPE of VVH. The native VVH (1 μg/ml; purified from culture supernatant of *V. vulnificus*), the WT (3 μg/ml), and the mutant (10 μg/ml) were incubated with CHO cells for 5 h at 37°C individually. (B) The mutant is expressed as a full-length VVH. The WT and the mutant were blotted with anti-His antibody or anti-VVH polyclonal antibody. Both the WT and mutant were found to be the same size with both antibodies.

The F334I mutant could not induce cytotoxicity in CHO cells. We next determined the cytotoxic activity of the F334I mutant in CHO cells by using the LDH release assay. LDH is an enzyme confined to the cytoplasm, and its extracellular presence reflects cell damage. The F334I mutant could not induce LDH release at the highest concentrations (7.2 μg/ml), even though the WT induced LDH release of 82.4 ± 3.7% at the same concentrations (Fig. 2). The rate of LDH release caused by the F334I mutant ranged from 0% to 5.2% throughout this experiment (Fig. 2). These results indicate that F334 is a critical residue for the cytotoxicity of VVH.

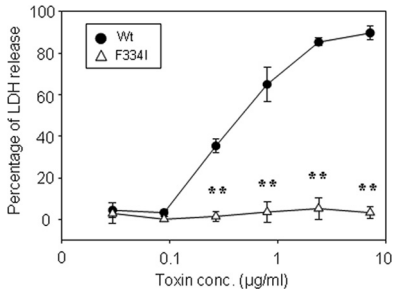

FIG. 2. The F334I mutant does not induce LDH release. CHO cells were incubated with various concentrations (conc.) of the WT or F334I mutant for 2 h at 37°C. The cytotoxic effects on CHO cells were assayed by the release of LDH. The results are expressed as a percentage of LDH release, as described in Materials and Methods. Data are presented as means ± standard deviations and represent three independent experiments, each in triplicate wells. **, significant decrease compared with the LDH release of the WT at the same concentrations (analysis of variance and Tukey's test, $P < 0.01$).

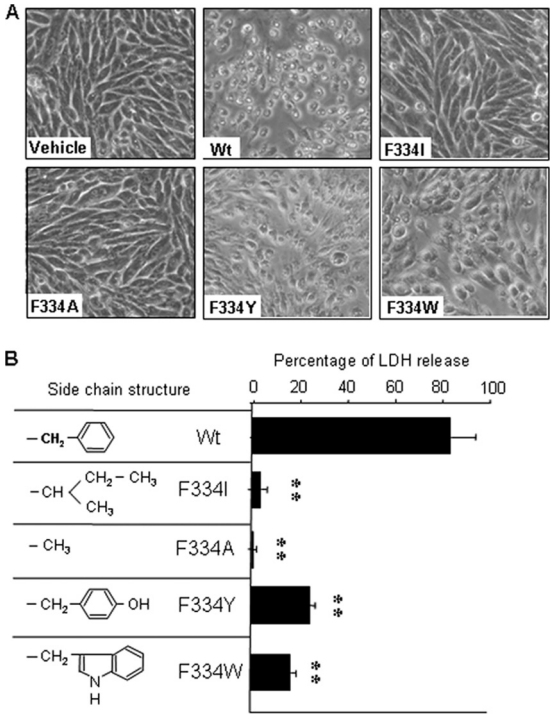

FIG. 3. The cytopathic and cytotoxic effect of F334 mutants on CHO cells. (A) CPE of F334 mutants. The CHO cells were incubated with the WT (3 μg/ml) and F334 mutants (3 μg/ml) for 5 h at 37°C individually. (B) Cytotoxicity of the WT and F334 mutants. The CHO cells were incubated with the WT (3 μg/ml) and F334 mutants (3 μg/ml) for 2 h at 37°C individually. The cytotoxic effects on CHO cells were assayed by the release of LDH. The results are expressed as a percentage of LDH release, as described in Materials and Methods. Data are presented as means ± standard deviations and represent three independent experiments, each in triplicate wells. **, significant difference compared with the LDH release of the WT (analysis of variance and Tukey's test, $P < 0.01$).

The aromatic ring of the 334th residue was needed for cytotoxicity of VVH. A benzene ring exists in a side chain of phenylalanine but is absent in isoleucine. We investigated the involvement of the benzene ring of F334 in cellular intoxication. To achieve this, three additional F334 mutants were generated by substitution of F334 to alanine (F334A), tyrosine (F334Y), and tryptophan (F334W). The tyrosine and tryptophan mutants (F334Y and F334W) have a benzene ring and indole ring in their respective side chains, while the isoleucine and alanine mutants (F334I and F334A) do not (Fig. 3B). As shown in Fig. 3A, F334A and F334I mutants could not induce CPE, and the level of LDH release from F334A or F334I mutant-treated cells was significantly reduced compared with that of the WT (Fig. 3B). On the other hand, both F334Y and F334W mutants caused a CPE and LDH release (Fig. 3A and B). Thus, we concluded that the aromatic ring at the 334th residue is needed for the cytotoxicity of VVH.

Hydrophobicity of the 334th residue was also needed for full cytotoxicity of VVH. Although F334Y and F334W mutants induced cytotoxicity, the percentages of LDH release of both mutants were lower than that of the WT (Fig. 3B). The side

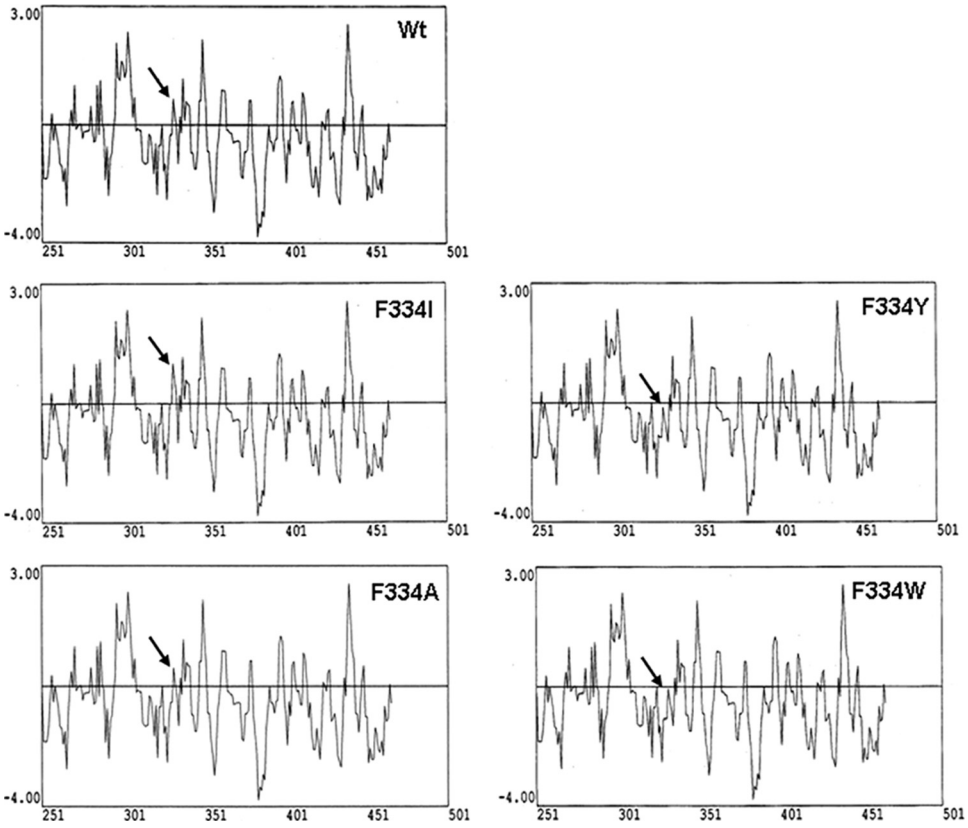

FIG. 4. The hydrophobicity around the 334th residue of F334 mutants. The hydrophobicity around the 334th residue of the WT and F334 mutants was analyzed using the parameter of Kite and Doolittle. Arrow indicates the hydropathy of the residue at position 334.

chain structures of phenylalanine and tyrosine are very similar, but tyrosine also has an additional hydroxyl group with a benzene ring in its side chain. Therefore, we next compared the hydropathy around the 334th residue in the series of F334 mutants by using the parameter of Kyte and Doolittle (14). Interestingly, both F334Y and F334W cytotoxic mutants are more hydrophilic than the WT (Fig. 4), whereas noncytotoxic F334I and F334A mutants have a level of hydrophobicity similar to that of the WT (Fig. 4). It seems likely that hydrophobicity of the 334th residue is not essential for cytotoxicity. However, even though both aromatic mutants (F334Y and F334W) could induce cytotoxicity, the levels of LDH release in both mutants were lower than that of the WT (Fig. 3B), suggesting that in addition to an aromatic ring, hydrophobicity of the 334th residue is also required for VVH to exert its full cytotoxicity. In other words, the first essential factor is an aromatic ring, and hydrophobicity of the 334th residue might be a secondary prerequisite. Of all amino acids, phenylalanine is the only one that has both an aromatic ring and hydrophobicity in its side chain. Therefore, VVH cannot exert its full cytotoxic ability if the F334 of VVH is replaced by any other amino acid.

Both the aromatic ring and hydrophobicity of F334 are essential for full binding activity. We showed that the benzene ring and hydrophobicity of F334 of VVH are critical to induce full cytotoxicity against CHO cells. Thus, we investigated the functional role of F334 in VVH cytotoxicity. It has been reported that the step of binding VVH to the cellular membrane is temperature independent, whereas oligomerization is temperature dependent (33). First, we investigated the binding activity of all mutants to CHO cells. Equal concentrations of the WT and the F334I, F334A, F334Y, and F334W mutants were incubated with CHO cells for 1 h at 4°C individually. At this temperature, only the binding of VVH to the cellular membrane occurred. As shown in Fig. 5, the values of intensity

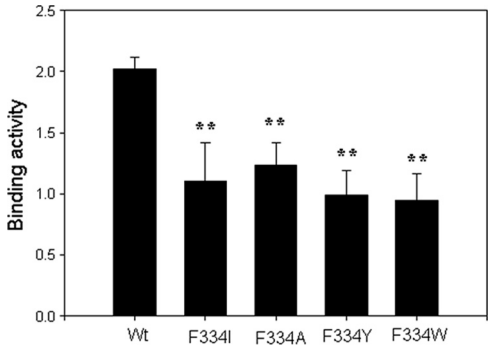

FIG. 5. Binding of F334 mutants to CHO cells. CHO cells were coincubated with the WT (20 μg/ml) and F334 mutants (20 μg/ml) for 1 h at 4°C individually. The binding activity of the WT and mutant were calculated as described in Materials and Methods. Data are presented as means ± standard deviations ($n = 3$). **, significant decrease compared with the binding activity of the WT (analysis of variance and Tukey's test, $P < 0.01$).

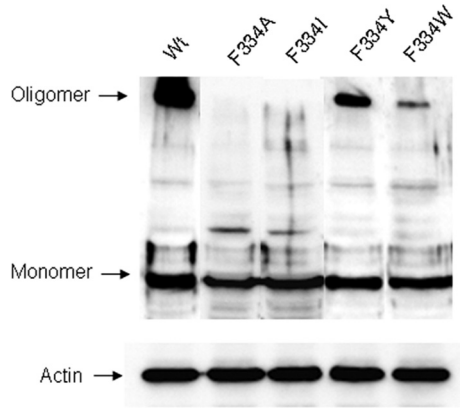

FIG. 6. Oligomerizing ability of F334 mutants on CHO cells. The WT (10 μg/ml) and F334 mutants (20 μg/ml) were incubated with CHO cells for 1 h at 37°C individually. The whole-cell lysates were subjected to SDS-PAGE followed by Western blotting with anti-VVH polyclonal antibody.

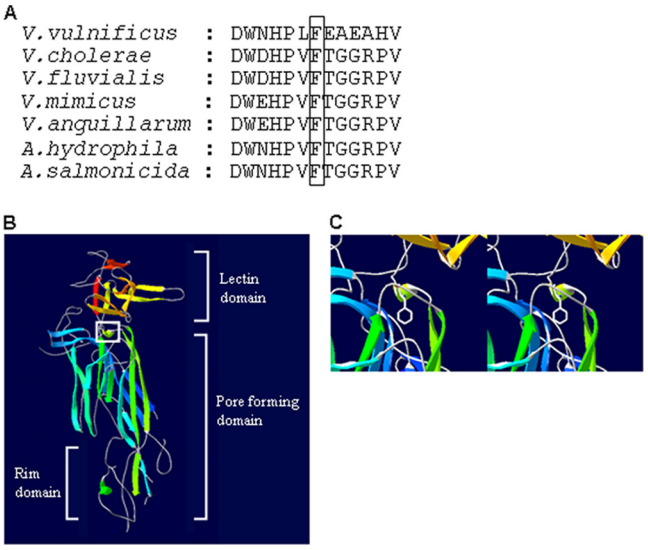

FIG. 7. Conservation and localization of F334. (A) F334 is conserved in other *Vibrionaceae* hemolysins. Box corresponds to F334 in VVH. (B) Localization of F334 on predicted three-dimensional structure of VVH. F334 sits on the short α-helix that is located between the lectin and pore-forming domains. (C) The side chain of F334 looks toward the inside of the pore-forming domain.

of the WT and the F334I, F334A, F334Y, and F334W mutants were 2.02 ± 0.10, 1.10 ± 0.32, 1.23 ± 0.19, 0.99 ± 0.20 and 0.95 ± 0.21, respectively. The binding abilities of all F334 mutants were reduced to approximately 50% compared with the WT (Fig. 5). Interestingly, there was no significant change in binding abilities between cytotoxic mutants (F334Y and F334W) and noncytotoxic mutants (F334I and F334A). These results indicate that both an aromatic ring and hydrophobicity of F334 were essential for full binding activity of this toxin. In addition, the differences in cytotoxicity among these mutants in spite of similarities in binding activity suggested that other mechanisms were involved in the reduction in cytotoxicity by these mutations.

Aromatic ring of 334th residue is critical for oligomerization in CHO cells. Despite an apparent decrease in the cytotoxicity of F334I and F334A mutants, both mutants could bind to CHO cells at a level similar to those of F334Y and F334W cytotoxic mutants (Fig. 5). Therefore, we investigated the oligomerization ability of the mutants on CHO cells. In this assay, all mutants were added in twofold concentrations of WT to get an equal amounts of binding toxin (Fig. 6). We confirmed that the binding amounts of the toxins were linearly increased in a concentration-dependent fashion. Oligomers of the WT and the F334Y and F334W mutants could be detected, whereas the oligomers of the F334I and F334A mutants could not (Fig. 6). Even when a threefold concentration of F334I was added to the cells, no oligomers of this mutant could be detected (data not shown). These data reveal that the aromatic ring of the 334th residue is essential for oligomerization of VVH. Although F334Y and F334W mutants are both aromatic mutants and have oligomerizing activity, the amount of oligomer is less than that of the WT. This result indicates that the aromatic ring at the 334th residue position is insufficient for full oligomerizing activity and that hydrophobicity may also be required.

F334 sits on the short α-helix that is located between the lectin and the pore-forming domains. We demonstrated that F334 was important for membrane binding and oligomerization of VVH (Fig. 5 and 6). To predict how F334 contributes to both binding and oligomerization in VVH, we modeled the three-dimensional structure of VVH by using the modeling server 3D-JIGSAW and analyzed the location of F334 in this model. The F334 sits on the short α-helix located between the lectin domain and the pore-forming domain (Fig. 7A). It is well known that hydrophobic residues, such as phenylalanine, are located inside molecules and contribute to the structural stability of protein (7, 23, 26, 29, 31). As expected, the side chain of F334 looks toward the inside of the pore-forming domain in this model of VVH (Fig. 7B).

F334 is highly conserved in other *Vibrionaceae* hemolysins. A BLAST search revealed that *Vibrio cholerae*, *Vibrio fluvialis*, *Vibrio mimicus*, *Vibrio anguillarum*, *Aeromonas hydrophila*, and *Aeromonas salmonicida* produced cytolysins/hemolysins related to those of VVH and have 28%, 28%, 27%, 30%, and 30% identity, respectively, at the amino acid level (data not shown). Although these are not high levels of identity, the phenylalanine residue that corresponds to position 334 of VVH is conserved in all of these cytolysins/hemolysins (Fig. 7C). This finding suggests that this phenylalanine may also play an important role in other *Vibrionaceae* cytolysins/hemolysins.

DISCUSSION

The overall toxic mechanism of VVH has been thought to be the same as those in other CDCs, but the structure-and-function relationships of VVH, including a site of binding to the cells and an oligomer formation site, are still unknown. We report here that the F334 residue of VVH, which is highly conserved in *Vibrionaceae* hemolysin, could influence the binding and oligomerization steps in the intoxication process of VVH. Furthermore, oligomerizing activity was dependent on an aromatic ring at residue 334.

We modeled the three-dimensional structure of VVH to

better understand the function of F334 in VVH. In our model, F334 sits on a short α-helix that is located at a site immediately adjacent to both the lectin and the pore-forming domain of VVH (Fig. 7A). Past studies of the structure-and-function relationships of leukocydin F (LukF) and staphylococcal α-hemolysin, which have structural similarity with VVH, showed that these toxins bind to the cellular membrane via the bottom of the rim domain (18, 28). For instance, LukF has a tyrosine residue at the bottom of the rim domain, and this tyrosine residue participates in the first attachment of LukF to the cellular membrane (34). It is also well known that the tryptophan-rich motif of gpCDCs, which is necessary to recognize and/or span the cellular membrane, exists at the bottom of the CDC protein (3, 9, 27). According to our model of VVH, some hydrophobic residues were present at the bottom of the rim domain (data not shown). Therefore, VVH would also bind to the cellular membrane via the rim domain. Although F334 is not located in the rim domain of VVH (Fig. 7A), it clearly affected binding activity on the cells (Fig. 5). One possible explanation for this is that the lectin domain is also involved in cell binding. Hazes reported that QxW triplet repeats (α, β, and γ) in the lectin domain are conserved in many carbohydrate binding proteins (8) and are also fully conserved in the VVH lectin domain (8, 21). It seems likely that the VVH lectin domain could participate in cell binding by recognizing a carbohydrate-containing molecule on the cellular membrane. The VVH lectin domain extends upward from F334 (Fig. 7B). It is also well known that VVH binds to cholesterol in vitro (10, 35), but the cholesterol binding site has not yet been defined. Interestingly, VVH does not have the tryptophan-rich motif that is highly conserved in gpCDCs and is involved in membrane recognition (3, 9, 27). Therefore, there is a great interest in understanding whether or not both cholesterol and carbohydrate are required for VVH to bind to susceptible cells. Further studies will be needed to define the cell binding mechanisms of VVH.

Mutation of F334 to Ile or Ala eliminated oligomerizing activity, whereas the Tyr and Trp mutants had oligomerizing activity. This result indicated that an aromatic ring at residue 334 was critical for oligomerization (Fig. 6). This may be explained by the localization of the F334 residue and by the direction of its side chain. As shown in Fig. 7C, the side chain of F334 in VVH looks toward the inside of the pocket, which is in the upper part of the β-sandwich in the pore-forming domain core (Fig. 7B). Song et al. found histidine-48 in the upper part of the β-sandwich and reported that it is a critical residue for cell binding in α-hemolysin (28). Moreover, hydrophobic residues are clustered in the upper part of the β-sandwich in LukF (20). These facts permit us to speculate that F334 participates in the structural stability of the β-sandwich in the pore-forming domain rather than being directly involved in the binding and oligomerization of VVH. However, to confirm this it will be necessary to perform a structural analysis to determine whether or not the aromatic ring of F334 plays a role in the stabilization of VVH structure. In addition, although the oligomers of the VVH F334Y and F334W mutants could be detected by Western blotting in our study, this finding should also be confirmed by pore formation in all mutants using other methods, such as single-channel recording (13, 16, 17).

Our findings will help in the design of future experiments to further our understanding of structure-and-function relationships in VVH and other *Vibrionaceae* hemolysins.

REFERENCES

1. **Bhakdi, S., J. Tranum-Jensen, and A. Sziegoleit.** 1985. Mechanism of membrane damage by streptolysin-O. Infect. Immun. **47:**52–60.
2. **Bhakdi, S., U. Weller, I. Walev, E. Martin, D. Jonas, and M. Palmer.** 1993. A guide to the use of pore-forming toxins for controlled permeabilization of cell membranes. Med. Microbiol. Immunol. **182:**167–175.
3. **Billington, S. J., J. G. Songer, and B. H. Jost.** 2002. The variant undecapeptide sequence of the Arcanobacterium pyogenes haemolysin, pyolysin, is required for full cytolytic activity. Microbiology **148:**3947–3954.
4. **Fromant, M., S. Blanquet, and P. Plateau.** 1995. Direct random mutagenesis of gene-sized DNA fragments using polymerase chain reaction. Anal. Biochem. **224:**347–353.
5. **Giddings, K. S., A. E. Johnson, and R. K. Tweten.** 2003. Redefining cholesterol's role in the mechanism of the cholesterol-dependent cytolysins. Proc. Natl. Acad. Sci. U. S. A. **100:**11315–11320.
6. **Gray, L. D., and A. S. Kreger.** 1985. Purification and characterization of an extracellular cytolysin produced by *Vibrio vulnificus*. Infect. Immun. **48:**62–72.
7. **Haga, K., R. Kanai, O. Sakamoto, M. Aoyagi, K. Harata, and K. Yamane.** 2003. Effects of essential carbohydrate/aromatic stacking interaction with Tyr100 and Phe259 on substrate binding of cyclodextrin glycosyltransferase from alkalophilic Bacillus sp. 1011. J. Biochem. **134:**881–891.
8. **Hazes, B.** 1996. The (QxW)3 domain: a flexible lectin scaffold. Protein Sci. **5:**1490–1501.
9. **Jacobs, T., M. D. Cima-Cabal, A. Darji, F. J. Méndez, F. Vázquez, A. A. Jacobs, Y. Shimada, Y. Ohno-Iwashita, S. Weiss, and J. R. de los Toyos.** 1999. The conserved undecapeptide shared by thiol-activated cytolysins is involved in membrane binding. FEBS Lett. **459:**463–466.
10. **Kim, B. S., and J. S. Kim.** 2002. Cholesterol induce oligomerization of *Vibrio vulnificus* cytolysin specifically. Exp. Mol. Med. **34:**239–242.
11. **Kim, H. R., H. W. Rho, M. H. Jeong, J. W. Park, J. S. Kim, B. H. Park, U. H. Kim, and S. D. Park.** 1993. Hemolytic mechanism of cytolysin produced from *V. vulnificus*. Life Sci. **53:**571–577.
12. **Krasilnikov, O. V., P. G. Merzlyak, V. L. Lima, A. O. Zitzer, A. Valeva, and L. N. Yuldasheva.** 2007. Pore formation by *Vibrio cholerae* cytolysin requires cholesterol in both monolayers of the target membrane. Biochimie **89:**271–277.
13. **Krasilnikov, O. V., P. G. Merzlyak, L. N. Yuldasheva, C. G. Rodrigues, S. Bhakdi, and A. Valeva.** 2000. Electrophysiological evidence for heptameric stoichiometry of ion channels formed by Staphylococcus aureus alpha-toxin in planar lipid bilayers. Mol. Microbiol. **37:**1372–1378.
14. **Kyte, J., and R. F. Doolittle.** 1982. A simple method for displaying the hydropathic character of a protein. J. Mol. Biol. **157:**105–132.
15. **Lowry, O. H., N. J. Rosebrough, A. L. Farr, and R. J. Randall.** 1951. Protein measurement with the Folin phenol reagent. J. Biol. Chem. **193:**265–275.
16. **Miles, G., H. Bayley, and S. Cheley.** 2002. Properties of Bacillus cereus hemolysin II: a heptameric transmembrane pore. Protein Sci. **11:**1813–1824.
17. **Miles, G., L. Movileanu, and H. Bayley.** 2002. Subunit composition of a bicomponent toxin: staphylococcal leukocidin forms an octameric transmembrane pore. Protein Sci. **11:**894–902.
18. **Montoya, M., and E. Gouaux.** 2003. β-Barrel membrane protein folding and structure viewed through the lens of alpha-hemolysin. Biochim. Biophys. Acta **1609:**19–27.
19. **Morgan, P. J., S. C. Hyman, A. J. Rowe, T. J. Mitchell, P. W. Andrew, and H. R. Saibil.** 1995. Subunit organisation and symmetry of pore-forming, oligomeric pneumolysin. FEBS Lett. **371:**77–80.
20. **Olson, R., H. Nariya, K. Yokota, Y. Kamio, and E. Gouaux.** 1999. Crystal structure of staphylococcal LukF delineates conformational changes accompanying formation of a transmembrane channel. Nat. Struct. Biol. **6:**134–140.
21. **Olson, R., and E. Gouaux.** 2005. Crystal structure of the *Vibrio cholerae* cytolysin (VCC) pro-toxin and its assembly into a heptameric transmembrane pore. J. Mol. Biol. **350:**997–1016.
22. **Palmer, M.** 2004. Cholesterol and the activity of bacterial toxins. FEMS Microbiol. Lett. **238:**281–289.
23. **Pless, S. A., K. S. Millen, A. P. Hanek, J. W. Lynch, H. A. Lester, S. C. Lummis, and D. A. Dougherty.** 2008. A cation-pi interaction in the binding site of the glycine receptor is mediated by a phenylalanine residue. J. Neurosci. **28:**10937–10942.
24. **Polekhina, G., K. S. Giddings, R. K. Tweten, and M. W. Parker.** 2005. Insights into the action of the superfamily of cholesterol-dependent cytolysins from studies of intermedilysin. Proc. Natl. Acad. Sci. U. S. A. **102:**600–605.
25. **Rossjohn, J., S. C. Feil, W. J. McKinstry, R. K. Tweten, and M. W. Parker.** 1997. Structure of a cholesterol-binding, thiol-activated cytolysin and a model of its membrane form. Cell **89:**685–692.
26. **Slutsky, M. M., and E. N. Marsh.** 2004. Cation-pi interactions studied in a model coiled-coil peptide. Protein Sci. **13:**2244–2251.
27. **Soltani, C. E., E. M. Hotze, A. E. Johnson, and R. K. Tweten.** 2007. Structural elements of the cholesterol-dependent cytolysins that are responsible for

their cholesterol-sensitive membrane interactions. Proc. Natl. Acad. Sci. U. S. A. **104:**20226–20231.
28. **Song, L., M. R. Hobaugh, C. Shustak, S. Cheley, H. Bayley, and J. E. Gouaux.** 1996. Structure of staphylococcal alpha-hemolysin, a heptameric transmembrane pore. Science **274:**1859–1866.
29. **Tatko, C. D., and M. L. Waters.** 2004. Comparison of C-H...π and hydrophobic interactions in a beta-hairpin peptide: impact on stability and specificity. J. Am. Chem. Soc. **126:**2028–2034.
30. **Tomita, T., M. Watanabe, and T. Yasuda.** 1992. Influence of membrane fluidity on the assembly of Staphylococcus aureus alpha-toxin, a channel-forming protein, in liposome membrane. J. Biol. Chem. **267:**13391–13397.
31. **van Herrikhuyzen, J., P. Jonkheijm, A. P. Schenning, and E. W. Meijer.** 2006. The influence of hydrogen bonding and pi-pi stacking interactions on the self-assembly properties of C3-symmetrical oligo(p-phenylenevinylene) discs. Org. Biomol. Chem. **4:**1539–1545.
32. **Yamamoto, K., A. C. Wright, J. B. Kaper, and J. G. Morris, Jr.** 1990. The cytolysin gene of *Vibrio vulnificus*: sequence and relationship to the *Vibrio cholerae* E1 Tor hemolysin gene. Infect. Immun. **58:**2706–2709.
33. **Yamanaka, H., T. Satoh, T. Katsu, and S. Shinoda.** 1987. Mechanism of haemolysis by *Vibrio vulnificus* haemolysin. J. Gen. Microbiol. **133:**2859–2864.
34. **Yokota, K., and Y. Kamio.** 2000. Tyrosine72 residue at the bottom of rim domain in LukF crucial for the sequential binding of the staphylococcal gamma-hemolysin to human erythrocytes. Biosci. Biotechnol. Biochem. **64:**2744–2747.
35. **Yu, H. N., Y. R. Lee, K. H. Park, S. Y. Rah, E. M. Noh, E. K. Song, M. K. Han, B. S. Kim, S. H. Lee, and J. S. Kim.** 2007. Membrane cholesterol is required for activity of *Vibrio vulnificus* cytolysin. Arch. Microbiol. **187:**467–473.
36. **Yuldasheva, L. N., P. G. Merzlyak, A. O. Zitzer, C. G. Rodrigues, S. Bhakdi, and O. V. Krasilnikov.** 2001. Lumen geometry of ion channels formed by *Vibrio cholerae* EL Tor cytolysin elucidated by nonelectrolyte exclusion. Biochim. Biophys. Acta **1512:**53–63.
37. **Zitzer, A., M. Palmer, U. Weller, T. Wassenaar, C. Biermann, J. Tranum-Jensen, and S. Bhakdi.** 1997. Mode of primary binding to target membranes and pore formation induced by *Vibrio cholerae* cytolysin (hemolysin). Eur. J. Biochem. **247:**209–216.
38. **Zitzer, A., E. J. Westover, D. F. Covey, and M. Palmer.** 2003. Differential interaction of the two cholesterol-dependent, membrane-damaging toxins, streptolysin O and *Vibrio cholerae* cytolysin, with enantiomeric cholesterol. FEBS Lett. **553:**229–231.